J Mater Sci

Growth of large-area, few-layer graphene by femtosecond pulsed laser deposition with double-layer Ni catalyst

Xiangming Dong[1,*], Shibing Liu[1], Haiying Song[1], and Peng Gu[1]

[1] Strong-field and Ultrafast Photonics Lab, Institute of Laser Engineering, Beijing University of Technology, Beijing 100124, China

Received: 10 August 2016
Accepted: 8 October 2016

ABSTRACT

We demonstrated a simple method of fabricating large-area, few-layer graphene that involves performing femtosecond pulsed laser deposition at a relatively low temperature of 500 °C and a high pressure of 10^{-5} Torr using a double-layer Ni catalyst. The average thickness of the resulting graphene films was less than 3 nm, their average area was more than 1 cm^2, and their electrical resistivity was only 0.44 mΩ.cm. The laser deposition process was also conducted at different laser energies, and it was observed that the quality of the few-layer graphene could be improved using a double-layer catalyst at a higher laser energy. The ejection of C clusters by breaking the C–C bonds of the HOPG through multi-photon ionization can explain the observed graphene formation characteristics. The insights may facilitate the controllable synthesis of large-area, mono-layer graphene and promote the commercialize application of the graphene.

Introduction

Graphene, with its planar sp^2-bonded honeycomb structure, is anticipated to contribute significantly to the development of next-generation electronics due to its promising material with excellent electrical properties [1, 2]. There are various methods of growing graphene films such as mechanical exfoliation [2], chemical vapor deposition (CVD) [3], and pulsed laser deposition (PLD) [4]. Among these techniques, PLD is a relatively simple and fast means of growing graphene films using vacuum technology and long pulse lasers, and it has become a popular of the aforementioned methods [5–7]. However, the high thermal effect induced by a long pulse laser induces the sputtering particle of large size, which results in the low quality of graphene films with poor electrical property and the increase of the experimental conditions, for example, high temperatures (>1000 °C) and low pressures (>10^{-6} Torr) [5]. Furthermore, the graphene films were obtained using a single-layer metal to increase the quality of graphene by PLD [6, 7]. However, the scale of graphene film was too small to provide bases for integrated device fabrication, and its electrical property was poor. In the contract, ultrafast short pulse laser (fs laser) can be used to perform film deposition precisely and efficiently [8, 9] and exhibit unique advantages over

Address correspondence to E-mail: xmdongxm@163.com

DOI 10.1007/s10853-016-0494-3

Published online: 18 October 2016

long pulse laser sources. High-energy supporting particles and atomic-sized matter clusters can also be induced due to the high peak powers of fs lasers and the multi-photon ionization of fs laser-ablated target materials [10], which result in the atomic level deposition of film and achieve the improvement of the film quality. Recently, the large-area, few-layer graphene had been deposited on substrate Si without catalyst[11]. The electrical property of graphene, which was obtained by single-layer and without catalyst Ni, is weak. So, it will limit the graphene applications with the electrical devices. In order to obtain the good electrical property and large-area graphene, the method with the double-layer Ni catalyst was introduced.

In this letter, we report the fabrication of large-area, few-layer graphene on a Si substrate by PLD at a relatively low temperature of 500 °C and a high pressure of 10^{-5} Torr, using double-layer Ni as the catalyst. Scanning electron microscopy (SEM), atomic force microscopy (AFM), an intensified charge-coupled device (I-CCD), X-ray diffraction (XRD), and a Raman spectroscope (RENISHAW, inVia Raman Microscope, 532 nm) were used to explore the properties of the few-layer graphene. In order to obtain ex situ Raman spectra of the interfacial graphene growth, the Ni films were partially etched away by hydrofluoric acid and de-ionized water.

Experiment

Preparation of graphene

Double laser beams were used to improve the work efficiency, as shown in Fig. 1a. Commercial HOPG and Ni were used as targets, a bare Si (1 0 0) wafer was employed as the substrate, and the distance between the targets and the substrate was 60 mm. In the deposition process, the irradiation source was an amplified Ti:sapphire fs laser, which provided 35 fs pulses of an energy of 3.5 mJ/pulse operated at a 1 kHz repetition rate and with a central wavelength of 800 nm. The PLD was performed at a substrate temperature of 500 °C, and the chamber was vacuumed to 10^{-5} Torr.

Preparation of double-layer Ni catalyst

Figure 1b–f show the fabrication steps used to obtain the large-area, few-layer graphene films. Firstly, the first Ni catalyst layer with a thickness of around 100 nm was deposited on the Si by PLD (Ni/Si), and the HOPG was irradiated to obtain a C film on first catalyst layer (C/Ni/Si). Then the second catalyst layer, again with a thickness of around 100 nm, was deposited on the C film. Thus, the double-layer catalyst had a sandwich structure (Ni/C/Ni/Si). Lastly, the HOPG was irradiated to deposit the few-layer graphene on the second-layer Ni. This experimental process was repeated using different laser energies.

Characterizations

X-ray diffraction (XRD) patterns were carried out using D8 Advanced XRD, Bruker AXS, Germany to investigate crystal composition of the samples Ni. The image of graphene film was observed by a SEM

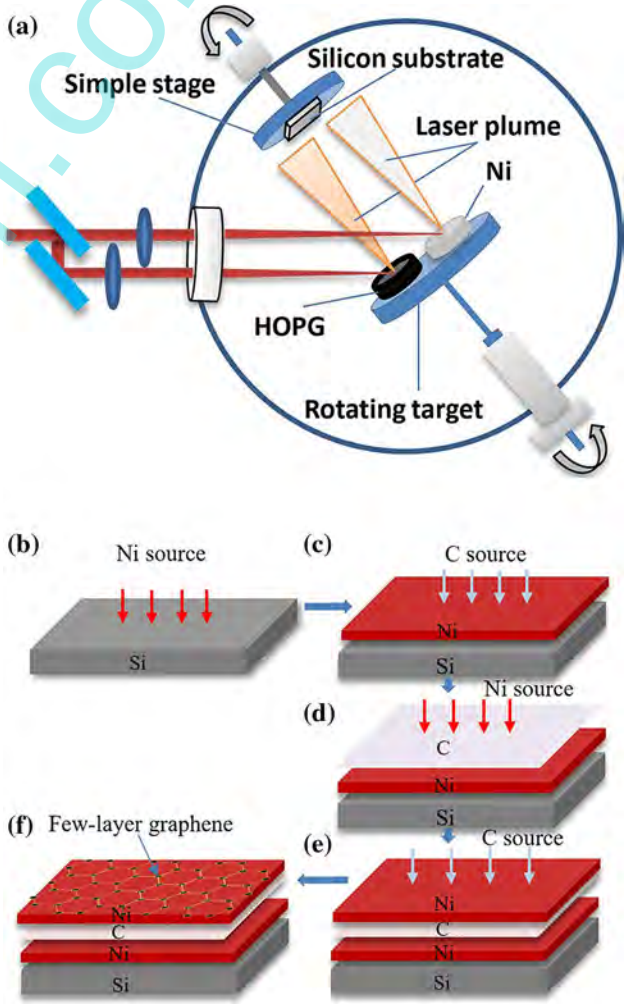

Figure 1 a Schematic image of laser deposition system; **b–f** fabrication steps used in few-layer graphene deposition.

(JEOLJSM 6500F, JEOL, Ltd.). The surface instruction of graphene and catalyst Ni was measured by AFM (CSPM 5000). The electrical resistivity of graphenes was measured by Hall Effect Sensor (HL5500). Raman spectroscopy was carried out on a RENISHAW, inVia Raman Microscope using a 532 nm laser. Optical spectra of samples were measured by I-CCD (PI-MAX3, Princetion Instruments).

Results and discussion

Figure 2a shows the Raman spectra of the graphene deposited on the Si on single- and double-layer Ni catalysts using a laser energy of 3 mJ, with a high-temperature (500 °C) annealing after the PLD step. The graphene spectra consist of three peaks, at 1350, 1580, and 2700 cm^{-1}. The G peak around 1580 cm^{-1} and the 2D peak near 2700 cm^{-1} are the most prominent Raman peaks of graphene [12], while the D peak near 1350 cm^{-1} results from disorder in the sp^2 carbon network [13]. The G peak is characteristic of the sp^2 structure and non-resonant scattering, reflecting the asymmetry and cleanliness. It occurs due to the in-plane vibrations of sp^2 either chain or ring form. The peak near 2700 cm^{-1} is the second-order D peak, which is generally referred to as the 2D peak. It arises from second-order zone-boundary phonons. The shapes of the 2D peaks of graphite and graphene exhibit clear differences. The 2D peak of graphite is not symmetric and has a shoulder peak at a slightly lower wave number. In contrast, the 2D peak of graphene is symmetric [7]. As such, the graphene films were deposited on our samples. The reduction of the 2D peak intensity results from an increased defect density, and the defect density of the graphene can be reduced with the decrease of the I_D/I_G [12, 14]. Correspondingly, the I_D/I_G of the film deposited on the double-layer Ni is found to be 0.32, while that of the film on the single-layer Ni is determined to be 1.03 (see Table 1). Meanwhile, I_{2D}/I_G of the sample on the single-layer Ni is determined to be 0.28, while that of the film on the double-layer Ni is found to be 1.4 (see Table 1). The intensity of the 2D peak is greater for the sample deposited on the double-layer Ni catalyst than for that deposited on the single-layer catalyst. Those differences indicate that fewer defects are present in the sample deposited on the double-layer Ni catalyst. The I_{2D}/I_G is often employed to determine the number of graphene layers [15], and the I_{2D}/I_G value of 0.69 for the film on the double-layer catalyst translates to 3–4 layers. Figure 2b presents an AFM image of the graphene film, showing its 2.06 nm thickness, and an SEM image of the graphene sheet with the smooth, featureless surface. Figure 2c and d show the topography of graphene film and Raman spectra at random locations in the patterned part of graphene, which show that the graphene is obtained uniformly on double-layer Ni, and the size of graphene is larger than the Reference [5]. The results demonstrate that the large area and uniform graphene is fabricated on the double-layer Ni.

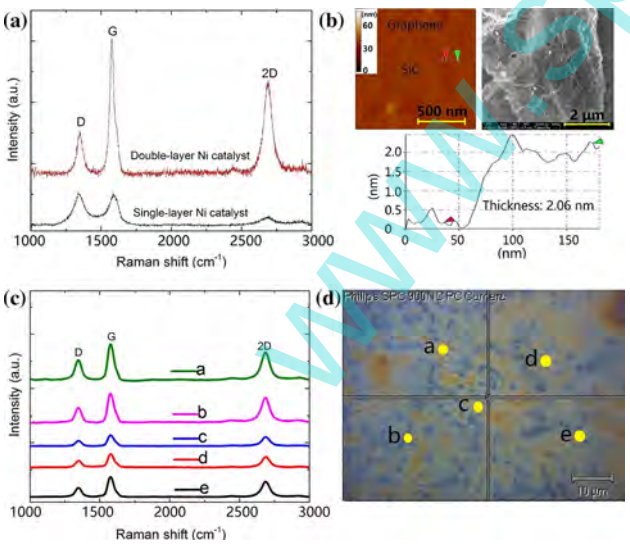

Figure 2 **a** Raman spectra of samples with single- and double-layer catalysts deposited at 3 mJ. **b** AFM and SEM images and cross-sectional measurements of graphene film deposited on double-layer catalyst using laser energy of 3 mJ, **c** 532 nm Raman spectra of 5 different locations, **d** Topography of the films formed on the substrate surface.

The electrical resistivity of graphene samples that had been transferred onto SiO_2/Si substrates were measured. The resistivity of the graphene film deposited on the double-layer catalyst is found to be 0.34 mΩ.cm (Measuring instrument: Hall Effect Sensor HL5500), which is lower than those previously

Table 1 Intensities and intensity ratios of D, G, and 2D peaks for films deposited on single- and double-layer Ni catalysts using laser energy of 3 mJ

Ni layer	I_D (a.u.)	I_G (a.u.)	I_{2D} (a.u.)	I_D/I_G	I_{2D}/I_G
1	506	493	137	1.03	0.28
2	692	2194	1524	0.32	0.69

reported for graphene films fabricated using CVD and PLD [14, 16]. The lower electrical resistivity of these graphene films make them ideal for use in various electronics applications. In the following, it was studied that the laser energy influenced the quality of the graphene film.

Figure 3 shows the Raman spectra of samples obtained with different laser energies, specifically, 1, 2, and 3 mJ. We find that I_D/I_G increases and electrical resistivity declines with the increase of laser energy (as seen in Table 2). This indicates that the graphene of the low defect density is obtained using a higher laser beam energy for laser deposition. Since the C–C bond energy of the ground electronic states in HOPG was previously estimated to be 3.7 eV [17], the 1.6 eV photon energy (corresponding to a wavelength of 800 nm) was not sufficiently high to break the C–C bonds and then deposit graphene. In fs laser deposition, the peak power irradiated onto the targets ranges from $1.9 \times 10^{14}\,W/cm^2$ to $5.7 \times 10^{14}\,W/cm^2$, and multi-photon ionization plays the leading role in the ablation process [18]. HOPG spectra were also obtained at energies of 1, 2, and 3 mJ, as shown in Fig. 4, by the I-CCD. A peak near 357 nm (3.5 eV) is evident in Fig. 4, which indicates that the C–C bonds in the HOPG were broken by the multi-photon ionization, resulting in the recombination of the C atoms on the Ni substrate, and then forming a crystalline structure with defect-free sp^2 rings. With increasing laser energy, the intensity of the peak near 357 nm also increases. Therefore, increasing the laser energy in PLD also improves the likelihood of breaking the C–C bonds and decreases the C cluster size [19], thereby promoting the formation of sp^2 rings on the Ni substrate. Thus, using a higher laser beam energy for laser deposition, the defect density of the resulting graphene film can be decreased.

We propose a qualitative explanation of the low defect density and large area of the graphene obtained using the double-layer Ni catalyst. The XRD patterns (Fig. 5e) show single-layer Ni and double-layer Ni film typically. There is no peak with first-layer Ni in the XRD spectrum, indicating the high surface roughness Ni is obtained. The XRD spectrum of polycrystalline Ni (second-layer), however, shows a Ni (111) and Ni (200) peak, which indicates the

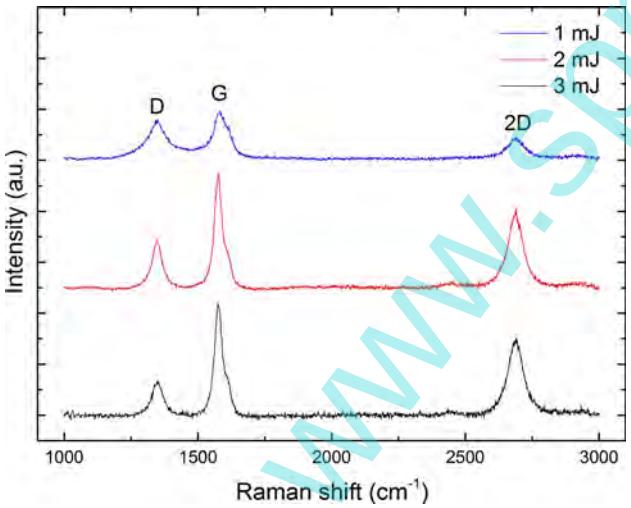

Figure 3 Raman spectra of samples deposited using different laser energies with double-layer Ni catalyst.

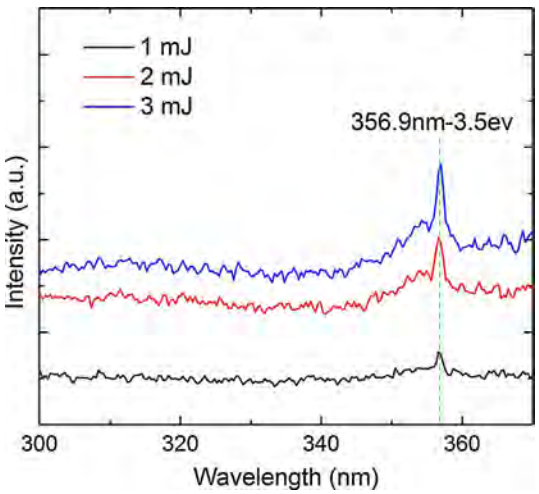

Figure 4 Optical spectra of samples deposited using different laser energies with double-layer Ni catalyst.

Table 2 Intensities and intensity ratios of D, G, and 2D peaks for films deposited at different laser energies on double-layer Ni catalyst

Laser energy (mJ)	I_D (a.u.)	I_G (a.u.)	I_{2D} (a.u.)	I_D/I_G	I_{2D}/I_G
1	771	921	411	0.84	0.45
2	689	1457	985	0.47	0.67
3	692	2194	1524	0.32	0.69

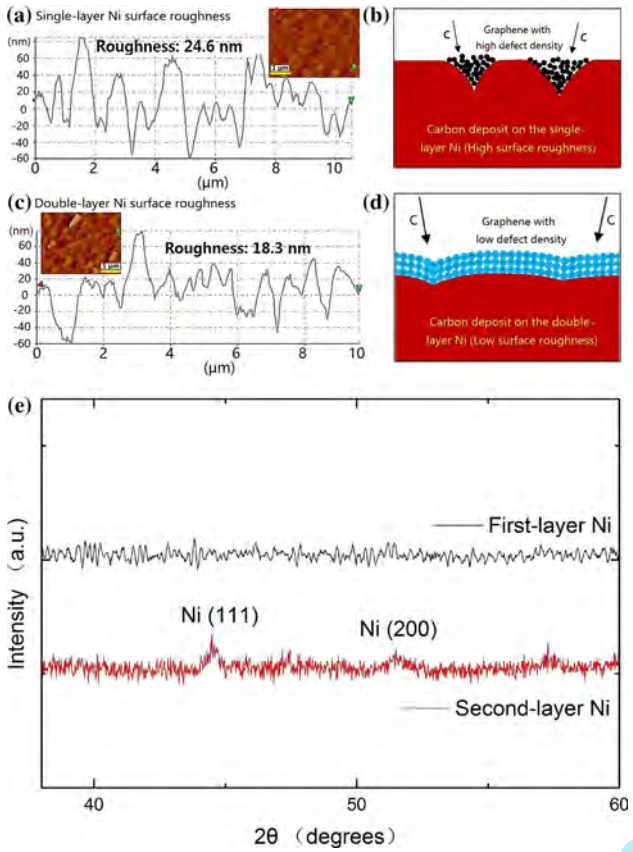

Figure 5 Cross-sectional measurements of roughnesses of **a** first and **c** second Ni catalyst layers and corresponding AFM images (*insets*); Schematic diagrams of graphene growth mechanism on the single-layer Ni (**b**) and the double-layer Ni (**d**). XRD patterns of first-layer Ni and second-layer Ni (**e**).

presence of second-layer Ni film grains with a smaller grain boundary. Fig. 5a and c present cross-sectional measurements of the surface roughnesses of the first and second layers of the Ni, respectively, while the insets depict AFM images of the catalyst layers. The surface of second-layer is considerably smoother (average roughness = 18.3 nm) than first-layer Ni (average roughness = 24.6 nm). After increase of Ni layer, the typical diffraction peak appears, which could be related to improve the quality and surface roughness, in good agreement with the results of XRD. According to the thermodynamics, the surface catalyst with little foreign atom can reduce the surface tension and promote the layered growth of the film, resulting in the decease of surface roughness [20]. In our experiment, for the single-layer Ni, the surface of Ni with high surface roughness has larger grain boundaries and surface tension, which make the accumulation of carbon at these sites during the dispersive phase and lead to the non-uniform distribution of film, resulting in the Volmer–Weber mode of C film. Therefore, the high defect graphene is obtained, as shown in Fig. 5b. In contrast, for the double-layer Ni catalyst, the first-layer C atom promotes the layered growth of the second-layer Ni and the crystal of Ni, which leads to the obtainment of the low roughness on the second-layer Ni surface. There are fewer inter-plane grain boundaries and surface tension on the surface of smoother Ni, allowing uniform dispersive of the C on the Ni surface and tending to the layer growth model, which result in enabling the formation of graphene films of high quality, as shown in Fig. 5d. Consequently, large-area and graphene films of low defect density are obtained using the double-layer Ni catalyst.

Conclusions

In conclusion, large-area, few-layer graphene of low defect density was obtained by fs PLD using a double-layer Ni catalyst. The first-layer C atom stimulates the growth of the lower roughness and fewer inter-plane grain boundaries on the Ni surface, and then the fewer inter-plane grain boundaries and surface tension with second-layer Ni promote, resulting in the production of large-area graphene with a low defect density and low electrical resistivity. The ejection of C clusters by breaking the C–C bonds of the HOPG through multi-photon ionization can explain the observed graphene formation characteristics. Fabrication of higher quality few-layer graphene was observed at a larger laser energy. These results will contribute to the understanding of the graphene growth mechanism and may facilitate the controllable synthesis of large-area, mono-layer graphene.

Acknowledgements

We gratefully acknowledge the support for this work from the National Natural Science Foundation of China (Grant No. 51275012)

References

[1] Geim AK (2009) Graphene: status and prospects. Science 324(5934):1530–1534

[2] Novoselov KS, Geim AK, Morozov SV, Jiang D, Zhang Y, Dubonos SV, Grigorieva IV, Firsov AA (2004) Electric field effect in atomically thin carbon films. Science 306:666

[3] Reina A, Jia X, Ho J, Nezich D, Son H, Bulovic V, Dresselhaus MS, Kong J (2009) Few-layer graphene films on arbitrary substrates by chemical vapor deposition. Nano Lett. 9:30

[4] Hemani GK, Vandenberghe WG, Brennan B, Chabal YJ, Walker AV, Wallace RM (2013) Interfacial graphene growth in the Ni/SiO2 system using pulsed laser deposition. Appl. Phys. Lett. 103:134102

[5] Zhang H, Feng PX (2010) Fabrication and characterization of few-layer graphene. Carbon 48:359–364

[6] Koh ATT, Foong YM, Chua DHC (2012) Comparison of the mechanism of low defect few-layer graphene fabricated on different metals by pulsed laser deposition. Diam Relat Mater 25:98–102

[7] Koh ATT, Foong YM, Chua DHC (2010) Cooling rate and energy dependence of pulsed laser fabricated graphene on nickel at reduced temperature. Appl. Phys. Lett. 97:114102

[8] Gaillard M, Boulmer-Leborgne C, Semmar N, Millon E, Petit A (2012) Carbon nanotube growth from metallic nanoparticles deposited by pulsed-laser deposition on different substrates. Appl Surf Sci 258:9237–9241

[9] Kant KM, Reddy NM, Rama N, Sethupathi K, Rao MSR (2006) Electrical transport and morphological study of PLD-grown nanostructured amorphous carbon thin films. Nanotechnology 17:5244–5247

[10] Johnson SL, Heimann PA, MacPhee AG, Lindenberg AM, Monteiro OR, Chang Z, Lee RW, Falcone RW (2005) Bonding in liquid carbon studied by time-resolved X-ray absorption spectroscopy. Phys Rev Lett 94:057407

[11] Dong X, Liu S, Song H, Gu P, Li X (2015) Few-layer graphene film fabricated by femtosecond pulse laser deposition without catalytic layers. Chin Opt Lett 13(2):021601

[12] Ferrari AC, Meyer JC, Scardaci V, Casiraghi C, Lazzeri M, Mauri F, Piscanec S, Jiang D, Novoselov KS, Roth S et al (2006) Raman spectrum of graphene and graphene layers. Phys Rev Lett 97:187401

[13] Dresselhaus MS, Jorio A, Hofmann M, Dresselhaus G, Saito R (2010) Perspectives on carbon nanotubes and graphene Raman spectroscopy. Nano Lett 10:751

[14] Kumar SRS, Alshareef HN (2013) Ultraviolet laser deposition of graphene thin films without catalytic layers. Appl Phys Lett 102:012110

[15] Reina A, Jia X, Ho J, Nezich D, Son H, Bulovic V, Dresselhaus MS, Kong J (2009) Large area, few-layer graphene films on arbitrary substrates by chemical vapor deposition. Nano Lett 9:30

[16] Vlassiouk I, Smirnov SN, Ivanov I, Fulvio PF, Dai S, Meyer H, Chi MF, Datskos P, Lavrik NV (2011) Electrical and thermal conductivity of low temperature CVD graphene: the effect of disorder. Nanotechnology 22(27):275716

[17] Houzumi S, Takeshima K, Mochiji K, Toyoda N, Yamada I (2008) Low-energy irradiation effects of gas cluster ion beams. Electron Commun Jpn 91:2

[18] Ager JW, Anders S, Anders A, Wei B, Yao XY, Brown IG, Bhatia CS, Komvopoulos K (1999) Ion implantation post-processing of amorphous carbon films. Diam Relat Mater 8:451

[19] Jeschke HO, Garcia ME, Bennemann KH (2001) Time-dependent energy absorption changes during ultrafast lattice deformation. Phys Rev Lett 87:015003

[20] Copel M, Reuter MC, Kaxiras E, Tromp RM (1989) Surfactants in epitaxial growth. Phys Rev Lett 63:632–639